

# Layer-by-layer assembly of a magnetic nanoparticle shell on a thermoresponsive microgel core

John Erik Wong<sup>a,\*</sup>, Akhilesh Krishnakumar Gaharwar<sup>a,b</sup>, Detlef Müller-Schulte<sup>c</sup>, Dhirendra Bahadur<sup>b</sup>, Walter Richtering<sup>a</sup>

<sup>a</sup>Institute of Physical Chemistry, RWTH-Aachen University, Landoltweg 2, 52056 Aachen, Germany

<sup>b</sup>Department of Metallurgical Engineering and Materials Science, Indian Institute of Technology—Bombay, Mumbai, India

<sup>c</sup>MagnaMedics GmbH, Martelenberger Weg 8, 52066 Aachen, Germany

Available online 19 December 2006

## Abstract

We describe the surface modification of magnetic nanoparticles (MNPs), the coverage of poly(*N*-isopropylacrylamide) (PNiPAM) microgel with the MNPs and the inductive heating of these carriers. PNiPAM surface itself was modified using the layer-by-layer (LbL) assembly of polyelectrolytes to facilitate the deposition of surface-modified MNPs. One advantage of this concept is it allows the tuning of the magnetic and thermoresponsive properties of individual components (nanoparticles and microgels) separately before assembling them. Characterisations of the hybrid core–shell are discussed. In particular, it is shown that (i) each layer is successfully deposited and, more importantly, (ii) the coated microgel retains its thermoresponsive and magnetic behaviour.

© 2006 Elsevier B.V. All rights reserved.

**Keywords:** Magnetic nanoparticle; PNiPAM microgel; Thermoresponsive; Layer-by-layer; Polyelectrolyte multilayer; Hybrid core–shell

Magnetic nanoparticles (MNPs) have unique, size-dependent properties. Composite or hybrid materials, essentially in the form of core–shell systems [1,2] are finding great interest in the field of biomedical applications such as drug delivery, separation and MRI [3–5]. For in vivo applications, three basic prerequisites have to be met: (i) the surface has to be compatible, (ii) non-toxic, and (iii) the particles must be well dispersed without forming agglomerates. This has stemmed the idea of using magnetic cores encapsulated in a protective shell. One rational approach is to embed nanoparticles in silica [6] because the latter can be readily functionalised to impart the protective shell. However, herein, we demonstrate the in situ preparation of MNPs in the presence of a polymer to provide protection and stability of the ferrofluid without the use of silica. The concept developed in the present paper is to then deposit these surface-modified MNPs as a shell on a thermoresponsive microgel core.

Thermoresponsive microgels have (i) high surface-to-volume ratios [7], high drug-loading capacities, and (ii) undergo fast, reversible structural changes from swollen to collapsed state by expelling the solvent, which therefore possess a release-trigger mechanism, making them potential candidates as remote controlled drug delivery vehicles [8]. Poly(*N*-isopropylacrylamide) (PNiPAM) is one of the most widely studied microgels [9]. It is non-hazardous, soluble in water, and has a lower critical solution temperature (LCST) around 32 °C, at which it undergoes a transition from a swollen hydrophilic to a collapsed hydrophobic state. If (drug loaded) PNiPAM is to be used in vivo, one has to devise a means to heat the microgel remotely above its LCST to release the drug. One way is to incorporate the MNPs in/on the microgel and to allow external manipulation of the microgel by a magnetic field to inductively generate enough in situ heat to cause the microgel to shrink. We describe the deposition of MNPs as a shell onto a PNiPAM core using the layer-by-layer (LbL) technique [10,11].

The LbL assembly is a very simple, versatile and one of the most important techniques of thin-film deposition. The

\*Corresponding author. Tel.: +49 241 8094750; fax: +49 241 8092327.  
E-mail address: [wong@pc.rwth-aachen.de](mailto:wong@pc.rwth-aachen.de) (J.E. Wong).

LbL involves the sequential adsorption of polyelectrolytes on a charged substrate. The thickness of each layer, consequently of the whole film, and the morphology, can be monitored and tuned down to Å precision by varying the ionic strength, type of salts, pH and temperature of the solutions from which these films are fabricated. These multilayered materials and structures may be developed with specifically tailored optical, magnetic, or electrical properties. The advantage of the LbL technique lies in the fact that there is no restriction in the shape or size of the substrates. Although most LbL assemblies have so far been performed on hard and rigid substrates, we recently reported the successful LbL assembly of polyelectrolyte multilayers on soft and porous thermoresponsive microgels [12,13]. It was already demonstrated that LbL can provide a successful pathway for fabricating inorganic and inorganic-hybrid structures [2,14]. The challenge now is to fabricate core–shell hybrid structures composed of MNPs on a soft and porous core.

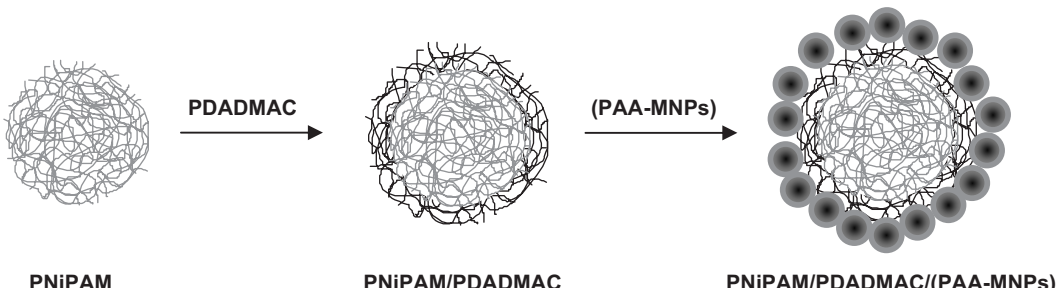
In this work, we report the incorporation of a surface-modified MNPs shell onto a PNiPAM core whose surface was modified with a polyelectrolyte sheath to facilitate the deposition of the MNPs (see Scheme 1). To the best of our knowledge, this is the first time that MNPs coating on thermoresponsive microgels is undertaken. This hybrid core–shell microgel offers a unique combination of thermoresponsivity and magnetism that could open up novel prospects for remotely controlled drug carriers. We describe first, the synthesis and characterisation of the MNPs, secondly those of the PNiPAM and finally those of the core–shell hybrid structure.

First, we set out to prepare negatively charged MNPs. The inclusion of the MNPs into a negatively charged polymeric shell (for example polyacrylic acid (PAA)) [15] in a solution containing the polymer [16] is one way to achieve this. Liao and Chen [17] prepared PAA-modified MNPs (PAA–MNPs) where PAA is covalently bound to the MNPs via carbodiimide activation *after* the MNPs were prepared. Here, we report the *in situ* preparation of MNPs *in the presence* of PAA. For this,  $\text{Fe}^{3+}$  solution was prepared by dissolving 0.81 g  $\text{FeCl}_3 \cdot 6\text{H}_2\text{O}$  (Sigma-Aldrich) in 5 ml water (all water used is double-distilled deionised water) and a  $\text{Fe}^{2+}$  solution was prepared by dissolving 0.4963 g  $\text{FeCl}_2 \cdot 4\text{H}_2\text{O}$  (Sigma-Aldrich) in a mixture of 1 ml water and 0.25 ml 37% HCl. Both solutions were placed in

an ultrasonic bath for 5 min to homogenise the mixture. The  $\text{Fe}^{3+}$  and  $\text{Fe}^{2+}$  solutions were then mixed and allowed to stand in the ultrasonic bath for a short time (about 2 min) just before the precipitation step. 0.1 g of PAA (Fluka,  $M_w = 5100 \text{ g/mol}$ ) was dissolved in 40 ml of water and 10 ml of 25%  $\text{NH}_3$  solution in a three-necked round bottom flask under an inert  $\text{N}_2$  atmosphere and constant stirring. To precipitate the iron oxide, the mixture of  $\text{Fe}^{3+}$  and  $\text{Fe}^{2+}$  was added dropwise to the PAA mixture under an inert atmosphere of nitrogen and continuous stirring. A black suspension was formed immediately and crystal growth was allowed to proceed for 30 min at room temperature with constant stirring to produce a stable, water-based suspension. Aggregates were first separated from the reaction mixture using a Nd–Fe–B magnet, and then washed three times with 0.3 M  $\text{NH}_3$  aqueous solution. Three cycles of centrifugation at 5000 rpm for 10 min were carried out and the precipitate was dissolved in 20 ml of water to obtain a stable ferrofluid. Exposure of this ferrofluid to a magnetic field revealed no phase separation, confirming the complete redispersion of the PAA–MNPs. A Zetasizer 3000HS (Malvern, UK) was used to characterise the PAA–MNPs. The PAA–MNPs has a zeta potential of  $-28 \text{ mV}$  and has a hydrodynamic radius of about 45 nm.

A crystallographic study of the iron-oxide powder was performed on a rotating anode STOE STADI-P X-ray diffractometer system using  $\text{CoK}_\alpha$  radiation ( $\lambda = 0.179026 \text{ nm}$ ). X-ray diffraction (XRD) graphics were compared to the JCPDS standard data in order to deduce the crystal structure of the product. The X-ray powder diffraction pattern of magnetite particles (Fig. 1(a)) showed a spinel phase. The precision of the XRD data was relatively low due to line broadening. The line positions and relative intensities were consistent with the presence of either magnetite or maghemite. The peaks were significantly broadened due to the small size of the crystallites. The volume average relative particle size of the crystal,  $D$ , was calculated using the Scherrer formula giving  $D_{311} \sim 14 \text{ nm}$ . Comparison of the data obtained from dynamic light scattering (DLS) and XRD gives an indication that the PAA–MNPs are not coated with single PAA layer, but merely a “defined aggregate” of several MNPs with probably several PAA chains.

Thermogravimetric analysis (TGA) on PAA–MNPs was carried out on the dried samples with a heating rate of



Scheme 1. LbL deposition of polyelectrolyte and magnetic nanoparticles on PNiPAM microgel.

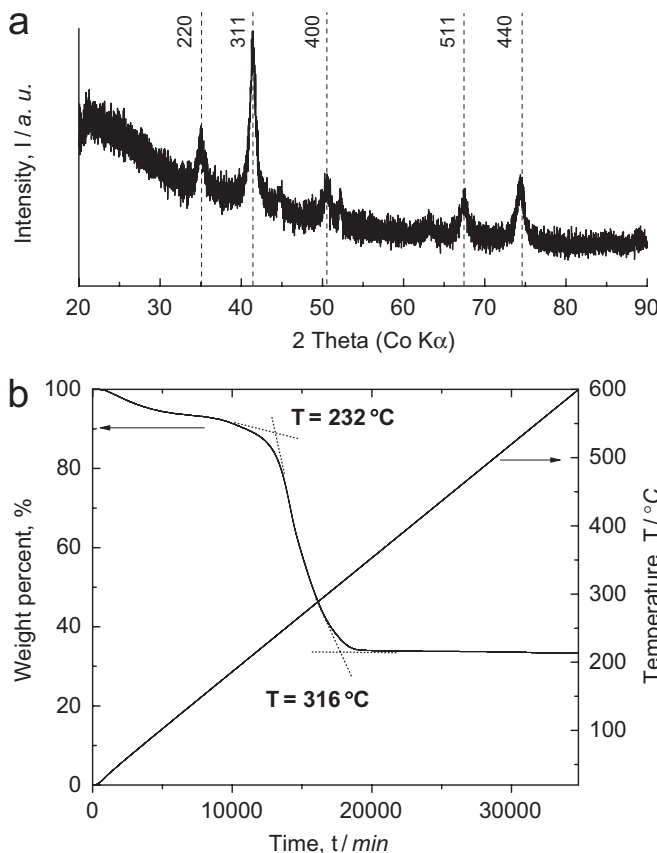


Fig. 1. (a) X-ray powder diffraction pattern of PAA–MNPs. (b) TGA curve showing % of weight loss and maximum temperature of decomposition of PAA–MNPs.

10 °C/min (from 20 to 600 °C), using a Setaram SETSYS thermogravimetric analyser in a nitrogen atmosphere. The TGA curve for PAA–MNPs, Fig. 1(b), revealed two steps in weight loss. The first step between 100 and 150 °C was due to the loss of residual water in the sample. The pronounced weight loss between 232 and 316 °C was due to the degradation of PAA [17]. There was no significant weight change between 316 and 600 °C, implying the presence of only iron oxide within the temperature range. This indicated that PAA was indeed bound to the MNPs. The concentration of PAA–MNPs in the ferrofluid was about 15.6%, as determined by drying the sample in an oven at 80 °C. From the percentage of weight loss in the TGA curve, the composition of the PAA–MNPs was estimated to amount to 33.3 wt% MNPs and 66.7 wt% PAA.

Magnetic properties were measured at room temperature using a superconducting quantum interference device (SQUID) magnetometer. The magnetisation curve reveals zero coercivity, zero remanence and the magnetisation does not saturate at 20 kOe revealing the superparamagnetic nature of the ferrite particles. The saturation magnetisation,  $M_s$ , was 45 emu/g at 20 kOe.

We then proceeded to synthesise the PNiPAM core microgel via free radical emulsion polymerization [18,19].

17.2175 g *N*-isopropylacrylamide (NiPAM) (Aldrich), 0.3275 g *N,N'*-methylenebis(acrylamide) (BIS) (Fluka), and 0.3275 g sodium dodecyl sulphate (SDS) (Fluka) were dissolved in 600 ml water at 72 °C under an inert atmosphere of nitrogen. 0.8750 g potassium persulphate (KPS) (Merck) was dissolved in 10 ml of water and added to the reaction vessel to start the reaction. The reaction was continued for another 5 h under nitrogen. This mixture was purified by three centrifugation cycles at 50,000 rpm (for 30, 20, and 15 min) using a Sorvall DiscoveryTM 90SE ultracentrifuge. The microgel was finally collected, redispersed in water overnight and filtered through a 1.2 μm filter.

The particle size of the thermoresponsive microgel was measured as a function of temperature by DLS. Light scattering experiments were carried out on highly diluted samples with an ALV goniometer (ALV 5000E correlator). Temperature was varied from 20 to 40 °C, in steps of 2 °C, in both directions, so that one complete cycle consisted of a heating curve followed by a cooling curve. Scattered light was detected at 60° and particles size was calculated by cumulant fits. Fig. 2(a) shows the DLS curve of PNiPAM, revealing (i) a hydrodynamic radius ( $R_h$ ) of 190 and 70 nm

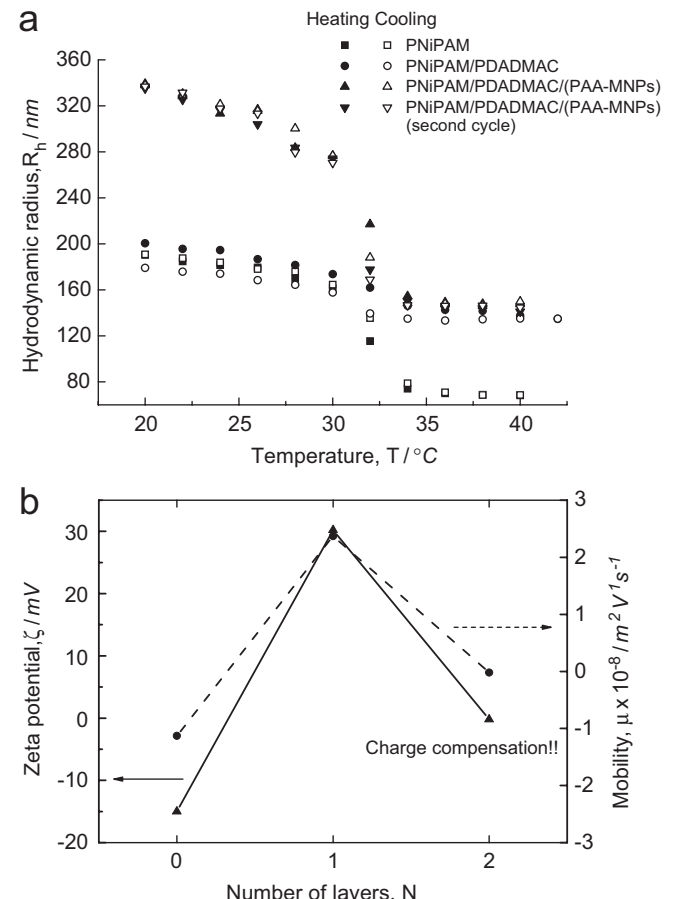


Fig. 2. (a) DLS curve of the uncoated PNiPAM, PDADMAC-coated PNiPAM, and the magnetic hybrid core–shell as a function of temperature; (b) electrophoretic measurements as a function of number of layers coated on the microgel.

in the swollen and collapsed state respectively, (ii) a completely reversible swelling and deswelling curves, and (iii) a LCST of around 32 °C.

The surface modification of PNiPAM was carried out using the LbL technique to deposit one layer of a positively charged polyelectrolyte, poly(diallyldimethylammonium chloride) (PDADMAC). 3 ml of a 1:100 diluted dispersion of microgels were added to 6 ml of a solution of 1 mg/ml PDADMAC (Sigma-Aldrich,  $M_w = 100,000$  g/mol) in 0.5 M NaCl to prepare a positively charged microgel surface. The solution was mixed for 24 h. The excess polyelectrolyte was removed, and the PDADMAC-coated microgel washed three times with water, by ultracentrifugation cycles at 50,000 rpm at 25 °C. In the final stage, the pure PDADMAC-coated microgel was redispersed in water overnight and filtered through a 1.2 µm filter. Fig. 2(a) shows the DLS curve for the PDADMAC-coated PNIPAM. On adsorption of the polyelectrolyte layer, the thermoresponsive behaviour of the microgel changes dramatically [12,13]. The layer of PDADMAC, results in an increase in size of the microgel. This increase is more noticeable in the collapsed state ( $T > LCST$ ). When the temperature is increased above the LCST, the tendency of the microgel core to collapse is restricted by the strong electrostatic attraction between the microgel and the PDADMAC layer. Consequently, in the collapsed state, the coated microgel is larger than the uncoated one [13] indicating the successful deposition of PDADMAC on the microgel.

To deposit the MNPs on the polyelectrolyte-coated microgel, a solution of PDADMAC-coated microgel was added slowly to a dilute solution of PAA-MNPs in a volume ratio of 1:5 and mixing was carried out for 24 h. The microgel coated with PAA-MNPs was separated from excess MNPs by magnetic separation. We observed that PAA-MNPs are very stable and do not form agglomeration in the presence of a magnetic field. But when the microgel coated with PAA-MNPs are exposed to a magnetic field, then these particles are attracted to the magnet very fast due to the higher magnetic dipole interaction between the MNPs present. The PAA-MNPs coated microgel was then washed three times with water using the above mentioned procedure at 25 °C and finally redispersed in water overnight.

DLS studies, Fig. 2(a), resulted in a hydrodynamic radius,  $R_h$ , of around 340 nm for the magnetic-coated microgel at 25 °C, and most importantly, revealed that thermoresponsivity is preserved. The swelling and deswelling of the hybrid composite is also completely reversible and reproducible as revealed by the two consecutive heating and cooling cycles during the DLS measurements. This indirectly shows that the PAA-MNPs do not detach from the microgel during the volume phase transition of the latter. This could be explained by the improved adhesion of the aggregate of PAA-MNPs (as compared to single MNPs with single PAA layer) to the surface-modified microgel. Fig. 2(b) shows the electrophoretic

measurements of the uncoated, polyelectrolyte-coated, and (PAA–MNPs)-coated microgel. The zeta potential alternates from −15 to +30 mV on addition of PDADMAC, revealing charge overcompensation necessary for charge reversal for further build up of multilayers. However, on addition of the negatively charged PAA–MNPs, there is charge compensation leading to an almost neutral zeta potential (−5 mV), indicating clearly that the PAA–MNPs are indeed deposited on the microgel. The expected size of the hybrid core–shell structure is 290 nm (obtained from the sum of the  $R_h$  (PDADMAC-coated microgel core) = 200 nm plus twice the  $R_h$  (PAA–MNPs) = 45 nm). This is consistent with the  $R_h$  obtained from DLS and also with the size obtained from the Philips CM 10 transmission electron microscopy (TEM) picture, Fig. 3. Due to the high accelerating voltage used in TEM (200 kV), polymeric network or polyelectrolyte chains are not visible on TEM micrographs. Instead, we observe a cluster-like structure of PAA–MNPs in a “flatten” circular geometry.

To basically show that a remotely control carrier system can be realised by an external stimulus, we performed inductive heating using a generator–oscillator combination (TIG 5/300, Hüttinger, Freiburg, Germany) with a maximum power dissipation of 5 kW. The coil-shaped and water-cooled antenna is made up of eight copper windings with an inner diameter of 20 mm and connected to a water-cooled resonance circuit that produces the electromagnetic field. The inductive heating tests were conducted using a field amplitude of 20 kA/m in combination with a frequency of 360 kHz. Inductive heating was performed in a glass tube (3 ml aqueous suspension volume) placed in the centre of the coil. The temperature of the suspension was measured by inserting an alcohol thermometer into the centre of the sample. Fig. 4 shows the rise in temperature of various concentrations of magnetic content (defined as the wt % of the magnetic core within the PAA–MNPs composition as determined by TGA) as a function of time.

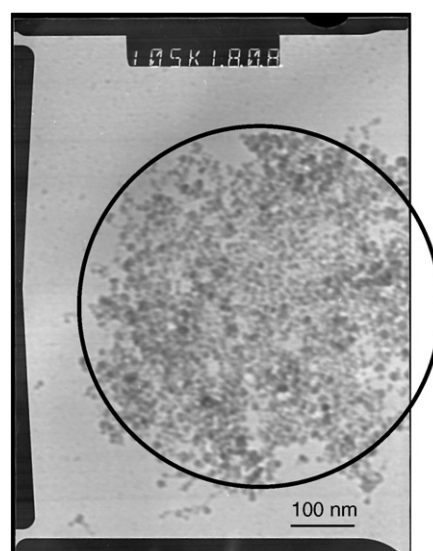


Fig. 3. TEM micrograph of PNiPAM/PDADMAC/(PAA–MNPs).

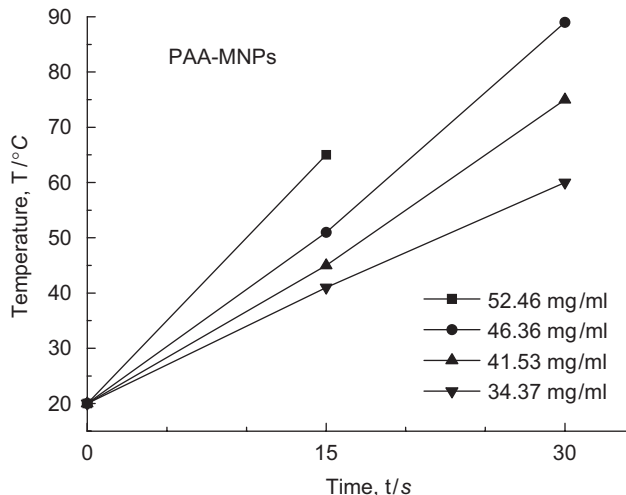


Fig. 4. Time-temperature curves of PAA–MNPs of different magnetic content when subjected to an alternating magnetic field (360 kHz, 20 kA/m).

From the inductive heating of the PAA–MNPs, it can be seen that these field parameters induce sufficient energy into the sample to reach temperature well above 50 °C in less than 30 s. Hence, we can conclude that the MNPs in the shell will generate enough heat to exceed the LCST of the PNIPAM core and cause the microgel to collapse.

We have demonstrated that it is possible to deposit a magnetic nanoparticles shell around a poly(*N*-isopropylacrylamide) core, whose surface has been modified by a layer of polyelectrolyte. Furthermore, this new hybrid core–shell microgel possesses a unique combination of thermoresponsivity and magnetism that could open up novel prospects for remotely controlled drug carriers.

## Acknowledgements

AKG would like to thank the Deutscher Akademischer Austauschdienst (DAAD) for a scholarship. D. Müller and D. Röhrens are thanked for TGA and XRD measurements, respectively, and Dr. M. Hodenius for the induction heating measurements. Support by the Fonds der Chemischen Industrie is gratefully acknowledged.

## References

- [1] L.M. Liz-Marzan, M. Giersig, P. Mulvaney, Langmuir 12 (1996) 4329.
- [2] F. Caruso, H. Lichtenfeld, M. Giersig, et al., J. Am. Chem. Soc. 120 (1998) 8528.
- [3] M.A. Willard, L.K. Kurihara, E.E. Carpenter, et al., Int. Mater. Rev. 49 (2004) 125.
- [4] T. Neuberger, B. Schopf, M. Hofmann, et al., J. Magn. Magn. Mater. 293 (2005) 483.
- [5] A. Jordan, R. Scholz, K. Maier-Hauff, et al., J. Magn. Magn. Mater. 225 (2001) 118.
- [6] Y.H. Deng, W.L. Yang, C.C. Wang, et al., Adv. Mater. 15 (2003) 1729.
- [7] B.R. Saunders, B. Vincent, Adv. Colloid Interface Sci. 80 (1999) 1.
- [8] D. Müller-Schulte, T. Schmitz-Rode, J. Magn. Magn. Mater. 302 (2006) 267.
- [9] R. Pelton, Adv. Colloid Interface Sci. 85 (2000) 1.
- [10] G. Decher, J.D. Hong, J. Schmitt, Thin Solid Films 210/211 (1992) 831.
- [11] G. Decher, Science 277 (1997) 1232.
- [12] N. Greinert, W. Richtering, Colloid Polym. Sci. 282 (2004) 1146.
- [13] J.E. Wong, W. Richtering, Prog. Colloid Polym. Sci. 133 (2006) 45.
- [14] F. Caruso, Adv. Mater. 13 (2001) 11.
- [15] J. Lee, T. Isobe, M. Senna, Colloids Surf. A 109 (1996) 121.
- [16] A.K. Fahlvik, J. Klaveness, D.D. Stark, J. Magn. Reson. Imaging 3 (1993) 187.
- [17] M.H. Liao, D.H. Chen, J. Mater. Chem. 12 (2002) 3654.
- [18] H. Senff, W. Richtering, J. Chem. Phys. 111 (1999) 1705.
- [19] H. Senff, W. Richtering, Colloid Polym. Sci. 278 (2000) 830.